Asymmetric Curvature of {110} Crystal Growth Faces in Polyethylene Oligomers

Goran Ungar* and Edy G. R. Putra

Department of Engineering Materials, University of Sheffield, Mappin Street, Sheffield S1 3JD, U.K.

Received January 24, 2001; Revised Manuscript Received May 9, 2001

ABSTRACT: Lamellar crystals laterally bounded by {110} faces only (nontruncated lozenges) are obtained from 1% octacosane solutions of alkanes *n*-dohexacontahectane ($C_{162}H_{326}$) and *n*-octanonacontahectane ($C_{198}H_{398}$) at the highest crystallization temperatures, i.e., 103 °C < T_c < 108 °C and 108 °C < T_c < 110 °C, respectively. This is in contrast with polydisperse polyethylene where {110}-bounded lozenges form only at low T_c. Crystals grown from 1-phenyldecane at the highest T_c are also nontruncated. However, while the crystals obtained from octacosane are faceted and rhombic, those grown from phenyldecane have their {110} faces asymmetrically curved at the obtuse apexes. This gives the crystals a leaf-shaped appearance, normally associated with {100}-bounded lamellae. To distinguish it from the established {100} bounded lenticular crystal morphology, the new habit is designated "*a*-axis lenticular". The particular type of curvature found for {110} faces is explained qualitatively by assuming a different rate of propagation in the two opposite directions of a new layer of stems. The "sharp" step travels faster, at a rate v_s, toward the acute apex, while the "blunt" step travels more slowly, at a rate v_b, toward the obtuse apex. The asymmetry is due to the absence of a mirror plane bisecting the {110} growth face.

Introduction

Polyethylene single-crystal lamellae grown from solution show a range of lateral habits, from rhombic lozenges at low crystallization temperatures T_c, through truncated lozenges, to lamellae elongated along the *b*-axis and often lenticular in shape at the highest T_c.[1,2] The edges of the lamellae are respectively {110}, {110}, {100}, and {100} crystal faces. In most cases the {100} faces are curved, while {110} are straight (faceted). There are indications that {110} faces may also become curved at high T_c, but at these temperatures they either disappear or become too short for their curvature to be studied. The situation with melt-grown crystals is broadly similar to that in crystals grown from solution at high T_c.[3,4]

The discovery of rounded crystal habits[5,6] has motivated Sadler to propose the rough-surface theory of crystal growth.[7] It was shown subsequently by Mansfield,[8] Toda,[2] and Point and Villers[9] that the curvature of {100} faces in polyethylene can be explained quantitatively by applying Frank's model of initiation and movement of steps.[10] Curvature occurs when the average step propagation distance is no larger than several stem widths, which places this type of crystal growth at the borderline between nucleated and rough-surface type. Rounded crystals have also been seen in other polymers,[11] but the curvature has only been analyzed for {100} faces in polyethylene.

The profile of {100} faces is symmetrical as a consequence of the existence of a mirror plane bisecting the crystal normal to these faces. However, such symmetry does not apply to {110}, and it would be of interest to investigate the shape of curved profiles of these faces if such profiles could be observed.

An opportunity to observe the entire profile of curved {110} faces has arisen in very long-chain monodisperse *n*-alkanes. Thus far, lenticular crystals with curved {100} faces have been observed in these compounds.[12] In fact, as found recently,[13−15] pure long alkanes display most if not all the crystal habits encountered in polyethylene. These habits accompany some rather dramatic changes in crystal growth kinetics, including the recently discovered negative order kinetics (acceleration by dilution)[13] and an associated effect termed "dilution wave".[13,16] In the present paper we report on the habits of crystals of alkanes $C_{162}H_{326}$ and $C_{198}H_{398}$ where, for the first time, we observe nontruncated {110} lozenges grown at high T_c. We then describe the appearance of curved {110} faces in such crystals which give rise to a new morphology, described as "*a*-axis lenticular". A tentative qualitative explanation of this crystal habit is proposed.

Experimental Section

The long-chain pure alkanes *n*-dohexacontahectane ($C_{162}H_{326}$) and octanonacontahectane ($C_{198}H_{398}$) were kindly provided by Drs. G. M. Brooke and S. Mohemmed of University of Durham, UK. The synthesis is described elsewhere.[17] The solvents 1-phenyldecane and *n*-octacosane were purchased from Sigma. Weighted amounts of the long alkane and the solvent were mixed and melted in small test tubes. After quenching to 0 °C the samples were stored in a freezer as solid suspensions. A small sample for optical microscopy was transferred onto a 6 mm coverslip, heated briefly to above the dissolution temperature of $C_{162}H_{326}$, and then covered with a preheated second slip. This procedure ensured the preservation of solution homogeneity. For rapid cooling to T_c a purpose-designed T-jump cell was used allowing T_c + 0.2 °C to be reached within 2 s by sliding the coverslip from the "hot" stage to a second stage preset to T_c centered on the light path. An interference contrast microscope was used with a long working distance 40× objective lens and a high-resolution CCD camera. Image time sequences were recorded by a frame grabber. Where crystallization was slower and longer isothermal runs were required, loss of solvent had to be prevented. This was achieved by using a conventional hot stage equipped with a purpose-built environmental cell allowing the maintenance of a saturated solvent vapor atmosphere. The gap between the coverslips is estimated to be 1−2 μm.

Results and Discussion

Change of Crystal Habit with Supercooling: General. In the case of $C_{162}H_{326}$ and $C_{198}H_{398}$ from octacosane we observe {110} faceted rhombic lozenges

10.1021/ma010146y CCC: $20.00
Published on Web 06/21/2001

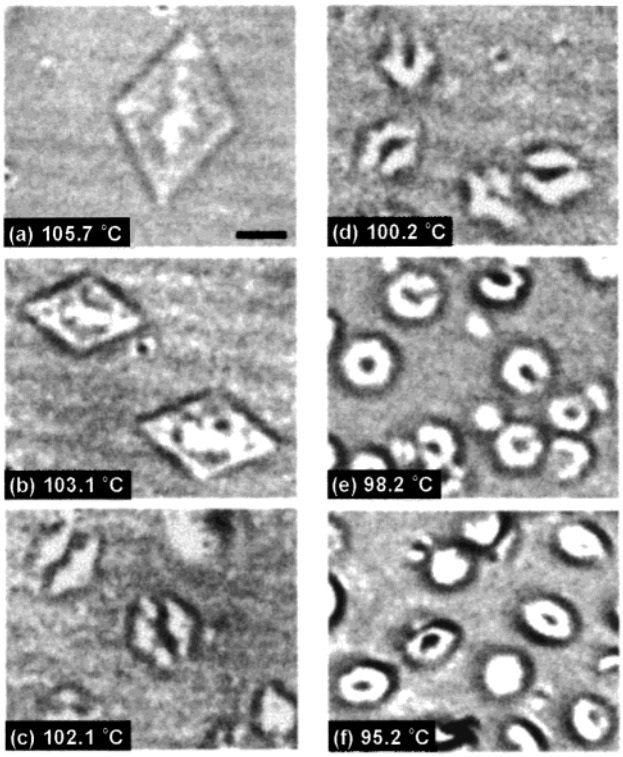

Figure 1. Extended-chain crystals of $C_{162}H_{326}$ in *n*-octacosane ($C_{28}H_{58}$) grown from an initially 1% solution at the temperatures indicated. Interference contrast optical micrographs. In this and subsequent micrographs the bar length represents 10 μm.

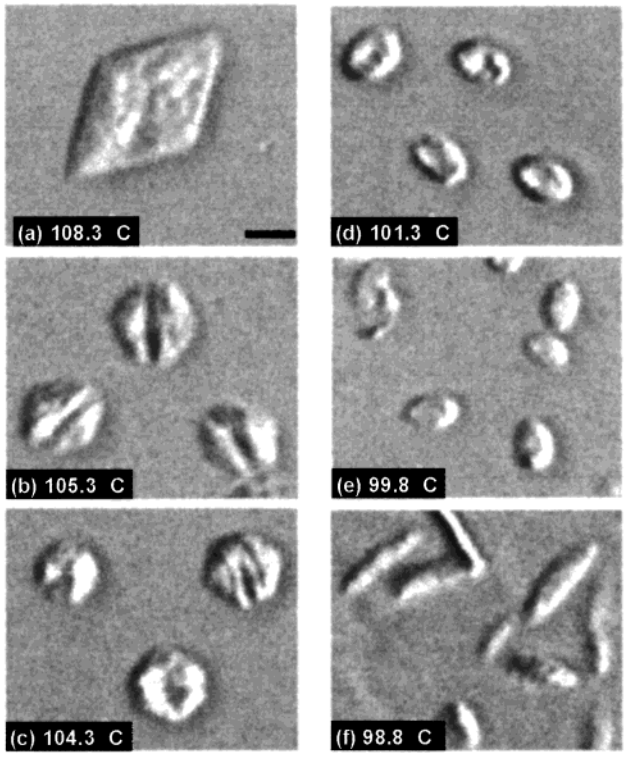

Figure 2. Extended-chain crystals of $C_{198}H_{398}$ in octacosane grown from an initially 1% solution at the temperatures indicated.

Table 1. Melting (T_m) and Final Dissolution Temperatures (T_d) of Extended (E) and Once-Folded (F) Form of *n*-Alkanes $C_{162}H_{326}$ and $C_{198}H_{398}$

	T_m^E (°C)	T_d^E (°C)	T_d^F (°C)
$C_{162}H_{326}$ pure	124.4		
in *n*-octacosane, 1%		108.5	
in 1-phenyldecane, 1%		102.1	85.7[a]
$C_{198}H_{398}$ pure	126.6		
in *n*-octacosane, 1%		111.3	98.3[a]
in 1-phenyldecane, 1%		106.0	95.3

[a] Measured on unannealed crystals.

at the highest T_c, i.e., above 103 °C for $C_{162}H_{326}$ (Figure 1a,b), and above 107 °C for $C_{198}H_{398}$ (Figure 2a). These temperature ranges correspond to respective supercoolings $\Delta T < 5.3$ °C and $\Delta T < 4.3$ °C which are only 16−21 °C below the melting temperature T_m (see Table 1). The angles of the rhombus correspond closely to crystallographic values: the acute angle is 66−68° for $C_{162}H_{326}$ and 64° for $C_{198}H_{398}$, compared to the crystallographic value of 67°. At lower T_c (Figures 1c−f and 2b−f) the lozenges become truncated by {100} faces. The crystals in Figures 1e and 2c are nearly hexagonal whereas those in Figures 1f and 2d−f are again elongated, progressively becoming leaf-shaped. These latter crystals are truncated lozenges described as type B[4] in polyethylene; i.e., they extend along the *b* axis and have long curved {100} faces and short {110} faces. In the case of $C_{162}H_{326}$ from octacosane crystallization at $T_c < 95$ °C was too fast to be recorded.

The faceted rhombic habit of crystals in Figures 1a,b and 2a indicate that {110} growth in octacosane at low supercooling can be safely regarded as nucleation controlled.

Figure 3 shows a sequence of optical micrographs of $C_{162}H_{326}$ crystals grown from 1% solution in phenyldecane at progressively lower T_c. Here, even for $C_{162}H_{326}$ it was possible to explore the entire range of extended-chain crystallization since growth takes place more slowly than in octacosane. For reference, the dissolution temperatures of extended and folded-chain crystals at 1% concentration are listed in Table 1. Where indicated, T_d^F has been measured on unannealed chain-folded crystals and is therefore an underestimate, as shown previously.[18]

Crystals grown from phenyldecane at the highest temperatures are not rhombic like those grown from octacosane. Instead, they are lenticular in shape (Figure 3a,b). However, these are not the lenticular crystals (type A) which form in polyethylene[3,4] or long alkanes[12] at high T_c and are bounded by two curved {100} faces and often have tapered ends; such crystals have their long dimension parallel to the *b*-axis. As seen in Figure 3c−e, the present "lenticular" crystals of $C_{162}H_{326}$ gradually become more angular and rhombus-like with decreasing T_c; the apparently smooth curved faces on each side of the "lenticular" crystals at $T_c > 98$ °C develop an apex in the middle. With T_c decreasing further the rhombus changes to an approximately hexagonal truncated lozenge shape (Figure 3f,g). Crystals of alkane $C_{198}H_{398}$ grown from 1% solution in phenyldecane follow the same pattern as those of $C_{162}H_{326}$ (Figure 4).

As T_c is lowered further (Figure 3h,i), the sequence of changing crystal habits becomes the same as that of crystallization from octacosane: Type B truncated lozenges are obtained, and with decreasing T_c, these become progressively more elongated along the *b*-axis. The succession of crystal shapes in Figure 3e−j is similar to those in Figures 1d−f and 2b−f. Lozenges with a progressively increasing degree of truncation by curved {100} faces can be recognized in Figures 1f, 2d,e, and 3f−i. The arrows in Figure 3g,h point to some of

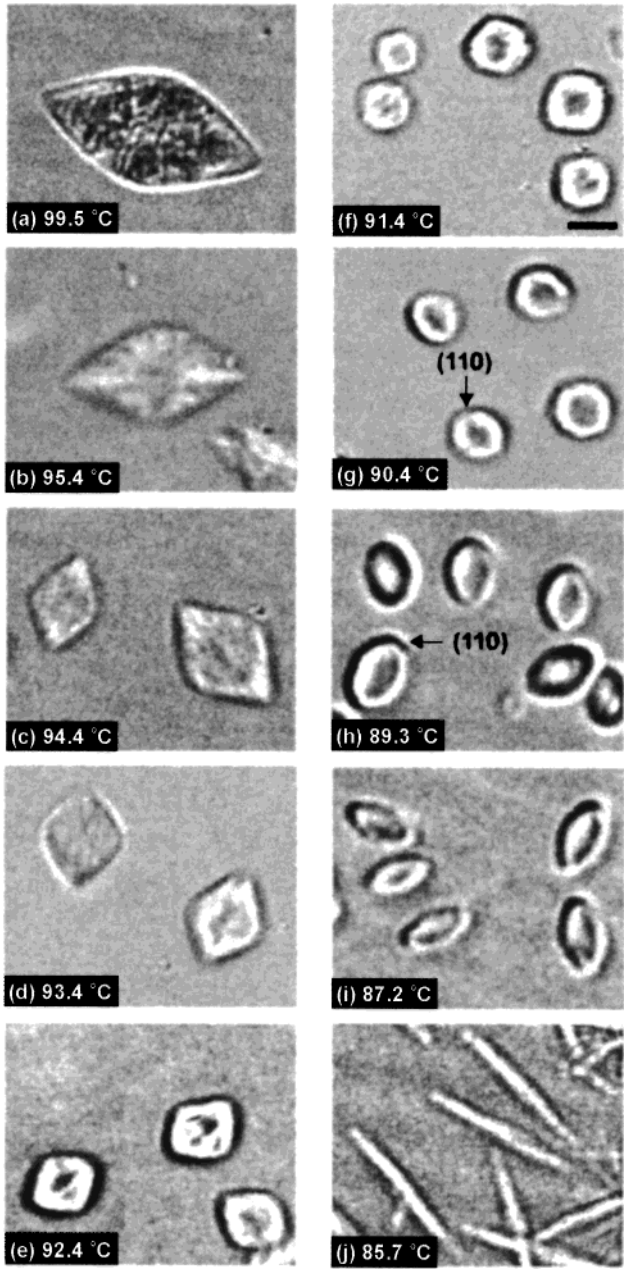

Figure 3. Extended-chain crystals of $C_{162}H_{326}$ in 1-phenyldecane grown from an initially 1% solution at the temperatures indicated.

the just discernible {110} faces of the type B crystals. With T_c decreasing still further (Figures 2f and 3i,j) the aspect ratio continues to increase until it reaches values of over 10:1 at the growth rate minimum, and the crystals assume a needlelike appearance.[14] At still lower T_c folded-chain crystals form (not shown).

From this behavior it is concluded that the rhombus-like crystals in Figures 3c−e and 4b are a variant of the commonly observed {110}-sectored lozenges, such as those in Figure 1a,b, but with somewhat altered apex angles (see below) and some rounding of the two obtuse apexes. It therefore follows further that the "lenticular" crystals at the lowest supercooling (Figures 3a,b and 4a) extend along the *a*-axis rather than the *b*-axis as in type A crystals and that the bounding face on each side is not a curved {100} face, but rather a combination of two merged curved faces best described as {110}.

In two aspects are the above crystal morphologies and their change with crystallization temperature unlike

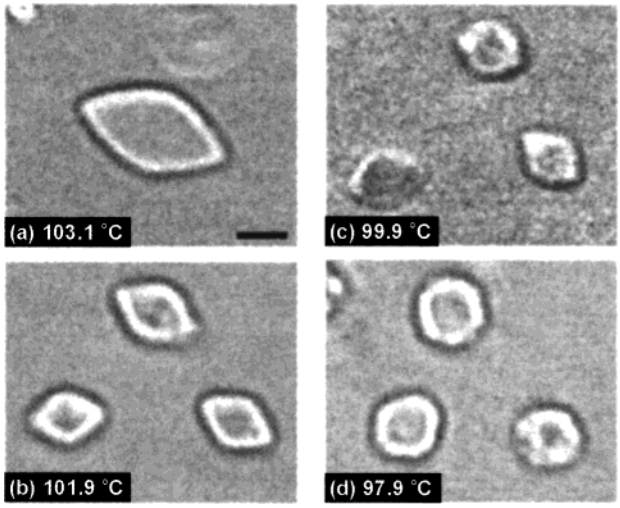

Figure 4. Extended-chain crystals of $C_{198}H_{398}$ in 1-phenyldecane grown from an initially 1% solution at the temperatures indicated.

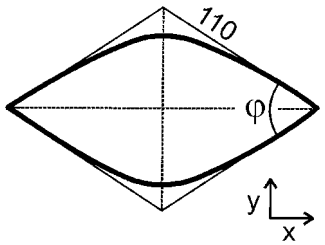

Figure 5. Outline of the crystal in Figure 3a.

any previously reported. The first unusual feature is the fact that the sequence of crystal habits with decreasing T_c (rhombic lozenge → truncated lozenge → increasing elongation along *b*-axis) is the exact reversal of the pattern for polyethylene, where such a sequence is observed with *increasing* T_c.[1,4,19] As argued elsewhere,[13,14] this change in morphology is associated with the self-poisoning effect.[20,21] The second intriguing feature is the "lenticular" shape, with the long dimension parallel to *a*-axis, observed in crystals grown from phenyldecane at low supercooling. This new morphology is the main topic of the present paper and is discussed below.

Observations on *a*-Axis Lenticular Crystals. The outline of the crystal in Figure 3a is redrawn in Figure 5. The crystal differs from a standard {110} lozenge in that its two obtuse apexes are rounded, while the acute ones remain sharp. In Figure 6 the average measured width-to-length ratio l_b/l_a of an average $C_{162}H_{326}$ crystal grown from phenyldecane is shown as a function of tan(φ/2) for different crystallization temperatures, where φ is the acute angle defined in Figure 5. For a lozenge-shaped crystal with straight lateral {110} faces l_b/l_a = tan(φ/2) (solid line); thus, the deviation of the experimental points in Figure 6 from the solid line is a measure of the extent of curvature at the obtuse apex. The trend is thus for a large radius of curvature at higher T_c. Conversely, the obtuse apex becomes more angular as T_c is lowered. This trend can also be discerned in the images in Figures 3 and 4. Figure 7 shows the angle φ for $C_{162}H_{326}$ crystals as a function of crystallization temperature T_c. It is at the highest T_c that φ is close to its ideal value of 67° calculated from

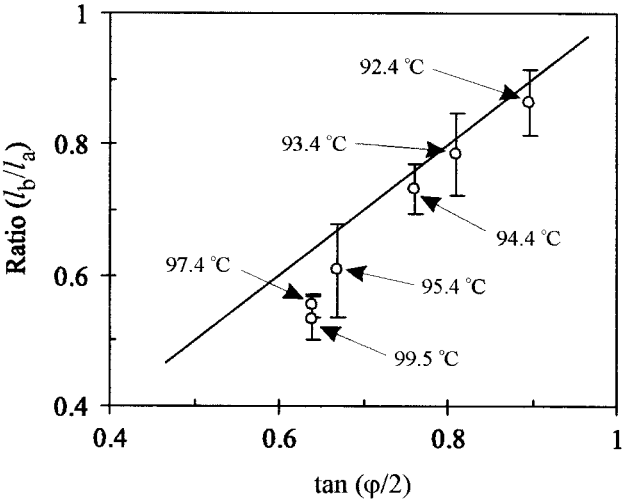

Figure 6. Plot of the crystal width-to-length ratio (l_b/l_a) against tan(φ/2) as defined in Figure 5. The symbol labels denote T_c. The solid line shows l_b/l_a vs tan(φ/2) for rhombic lozenges with perfectly straight edges.

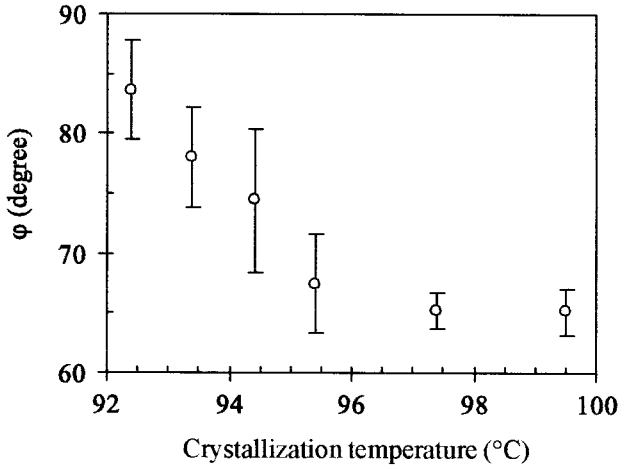

Figure 7. Dependence of the acute angle φ for phenyldecane-grown crystals of $C_{162}H_{326}$ on crystallization temperature. The value of φ for an ideal {110} lozenge crystal is 67°.

the unit cell dimensions. Below $T_c = 96$ °C φ increases significantly.

Curvature of the 110 Face. In the following we try to rationalize the observed morphology of *a*-axis lenticular crystals of $C_{162}H_{326}$ and $C_{198}H_{398}$. This is done in a qualitative way, and no attempt is made here at obtaining a mathematical solution.

Previous treatments of curved lamellar edges have all referred to the {100} faces of polyethylene crystals. They start with the model of Frank[10] in which a nucleation event creates a pair of steps. The nucleation rate is i per unit of edge length and time, and the steps travel to the left and to the right at an average net rate v (length per unit time). In the vicinity of position x along the substrate of length L the average densities of left and right steps are respectively $l(x)$ and $r(x)$. Two differential equations must therefore be satisfied at x:

$$\partial l/\partial t = i + v(\partial l/\partial x) - 2vlr \quad (1a)$$

$$\partial r/\partial t = i - v(\partial r/\partial x) - 2vlr \quad (1b)$$

where the last term on the right represents the step annihilation rate.

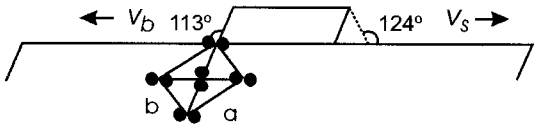

Figure 8. Top view of a new molecular layer deposited on a 110 growth face showing the asymmetry of steps. A unit cell is shown for reference.

At the ends of the substrate at $x = \pm L/2$, assuming that no steps enter from outside, the boundary conditions are

$$l_{(L/2)} = r_{(-L/2)} = 0 \quad (2)$$

In real crystal growth the substrate length increases simultaneously with the advance of the growth front. Thus, the substrate ends move outward at a net rate h. Mansfield,[8] Toda,[2] and Point and Villers[9] have obtained solutions of the above equations with moving boundaries, deriving the growth face profile $y(x,t)$. Such $y(x,t)$ describes adequately the observed and simulated[22] shapes of {100} faces of single crystals of polyethylene and, as found recently,[14,15] long alkanes, too. $y(x)$ defines an ellipse if a square lattice is used,[8] even though this is not strictly true for very small crystals.[9] The ellipse becomes leaf-shaped when transposed onto a polyethylene-like centered rectangular lattice.[4] According to the approximate treatment,[8] the {100} face is given as part of this ellipse when the substrate boundary $L/2$ moves at a rate $h < v$,[8] i.e., in the case of truncated lozenge. In the case of the {100} growth face, h is determined by G_{110}, the growth rate of the {110} face. On the other hand, if $h > v$, the outer parts of the {100} face are described by straight noncrystallographic edges tangent on the central elliptical section.[2,9]

We suggest that the key to understanding the curved {110} faces of the present *a*-axis lenticular crystals of $C_{162}H_{326}$ and $C_{198}H_{398}$ is to assume that the rates of propagation of left and right steps are different. Figure 8 illustrates the difference between the "sharp" (right) and the "blunt" (left) step. If the lattice had hexagonal symmetry, there would be no difference between the steps or between their propagation rates; the right and the left steps would be equivalent, both having an angle of 120°. However, in the orthorhombic lattice of polyethylene the two step angles differ by 11° (see Figure 8). Similarly, the distance between adjacent chains in the {100} plane (length of the dashed right-hand edge) is shorter than the distance in the {110} plane (length of the left-hand edge). These differences would be expected to produce some difference in either the molecular attachment or detachment rates, or both. We performed a molecular mechanics calculation of van der Waals interaction energies for *n*-alkane (*n*-octane) chains at each end of a row on a {110} face and found no significant difference between them. While this would suggest similarity in detachment rates, it is reasonable to expect that a difference in attachment rates would be caused by the difference in step angles (124° on the right vs 113° on the left; see Figure 8).

With reference to Figure 8, eqs 1a and 1b now become

$$\partial l/\partial t = i + v_b(\partial l/\partial x) - (v_b + v_s)lr$$

$$\partial r/\partial t = i - v_s(\partial r/\partial x) - (v_b + v_s)lr$$

It is the obtuse rather than the acute apexes of the crystal that are rounded, and this leads us to conclude

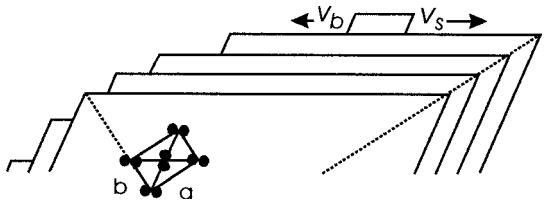

Figure 9. Schematic representation of a 110 growth face of a leaf-shaped {110}-bounded crystal illustrating the origin of the curved obtuse apex (left) and the sharp acute apex (right). Several outer molecular layers are shown. Dotted lines represent sector boundaries.

that $v_s > v_b$. The argument is illustrated schematically in Figure 9. Consider the top layer. A new nucleus can form anywhere on its surface, but if it spreads to the right faster than to the left, the curvature at the right end of the growth face will be less pronounced. In fact, at low supercooling there is only a slight curvature at the acute apex of the crystals (Figure 3a−c), meaning that even close to the end of the substrate $\partial r/\partial x \cong 0$. This means that the layers do not pile up at the right end of the substrate. With reference to the initiation rate i, v_s is relatively high, and on the right-hand side, the growth of the crystal has the hallmarks of a predominantly nucleation-controlled process.

In contrast, on the left-hand side near the obtuse apex of the crystal, the observed curvature indicates that there is significant pileup of layers. This means that step propagation rate to the left (v_b) is slow. In cases of {100} growth where v is low it is normal that the imbalance $\partial < l$ occurs near the left end of the substrate; this is a consequence of fewer nucleation events to the left of x compared to the number of events to the right of x. However, in the present case of {110} growth this imbalance is exacerbated further by the right-hand steps drifting to the right more rapidly and annihilating.

As seen from the graph in Figure 6 and from the micrographs in Figure 3, the curved portion of the {110} faces at the obtuse apex diminishes with increasing supercooling, thus giving the crystals a more faceted appearance. One possible reason for this may be a reduction in the relative difference between v_b and v_s caused by increasing supercooling. This relatively weak effect may suggest that the difference between v_b and v_s may be caused to some extent by a difference in chain detachment rates B, as these, rather than the attachment rates, are affected by supercooling ΔT through

$$B \propto \exp\left(-\frac{abl\Delta S}{kT\Delta T}\right) \quad (\Delta S \text{ is the entropy of fusion})$$

The Value of Angle φ. As already mentioned, the magnitude of angle φ at the acute apex is close to the crystallographic value of 67° for 96 °C < T_c < T_m in the case of $C_{162}H_{326}$. However, below 96 °C φ increases steadily to reach 84° at T_c = 92.4 °C (Figure 7). Below this temperature optical micrographs (Figure 3) show the appearance of {100} faces; i.e., the crystals become truncated lozenge shaped. The constant crystallographic value of φ above 96 °C is consistent with predominantly nucleation-controlled growth, leading to nearly crystallographic lateral facets with few steps. As suggested above, this is a consequence of relatively high v_s in relation to i.

Although {100} faces become visible only at around 92 °C, there is a possibility that the onset of the increase in φ around 96 °C coincides with the first emergence of {100} sectors which are too narrow to be observed by optical microscopy. In favor of this interpretation is the observation that crystals grown at T_c < 96 °C often display a streak along the long diagonal (Figure 3), i.e., where the {100} sector is expected.

{100} sectors should emerge at a supercooling at which $G_{100} = h < v_s$. Although in the approximate treatment of Mansfield[8] the presence of substrate edge does not affect the shape of the growth profile $y(x)$, in the more general treatment of Point and Villers (see section 6.3 of ref 9) the slope of the "elliptical" segment at the substrate end, $|dy/dx|$, indeed increases as the ratio h/v decreases below 1.

The Effect of Solvent. Finally, the experiments show that the nature of the solvent has a noticeable effect on the shape of {110} growth faces. While {110}-bounded crystals from phenyldecane display pronounced curvature, such crystals grown from octacosane have straight {110} edges at all temperatures at which they form (Figures 1 and 2)—this despite their T_c being 6 °C higher (see Table 1). Crystals grown from octacosane have sharp apexes with their angles having crystallographic values. This indicates that, with reference to i, the step spreading rates v_s and v_b are both high. Thus, {110} growth in octacosane can be regarded as truly nucleation-controlled. It was indeed found that the overall growth rate G_{110} for alkane $C_{162}H_{326}$ in octacosane is higher by a factor of 3 compared to that in phenyldecane at the same supercooling.[14] This indicates that in phenyldecane the step spreading rate is inhibited to a larger extent than in octacosane.

The effect of solvent does not appear to be related to self-poisoning, since we are dealing here with crystallization close to the extended-chain dissolution temperature. For $C_{162}H_{326}$ this is 16 °C above the transition temperature between extended and once-folded chain crystals (Table 1). Thus, there are no processes in significant competition with extended chain deposition.

Conclusions

Below are the main results of this work:

(i) Crystal lamellae bounded exclusively by {110} lateral faces can be grown from solution at high temperatures and low supercooling by using monodisperse *n*-alkanes $C_{162}H_{326}$ and $C_{198}H_{398}$.

(ii) While faceted nontruncated rhombic crystals grow from octacosane, similarly nontruncated {110}-bounded crystals are formed from phenyldecane, but with their {110} faces asymmetrically curved at the obtuse apexes. As a consequence, their appearance is similar to the lenticular Type A crystals of polyethylene grown at high T_c, except that their long dimension is parallel to the crystallographic a-axis.

(iii) To explain the curvature of {110} faces, we assume a different rate of propagation in the two opposite directions of a new layer of stems on a {110} growth face. The "sharp" step travels faster, at rate v_s, toward the acute apex, while the "blunt" step travels more slowly, at rate v_b, toward the obtuse apex.

(iv) The increase in angle φ of the acute apex above its crystallographic value, occurring at T_c < 96 °C in $C_{162}H_{326}$, is attributed to the appearance of submicroscopic {100} sectors acting as slow-growing substrate for {110} faces.

(v) In both phenyldecane and octacosane as solvents the extended-chain crystal morphology changes with increasing supercooling from {110}-bounded lozenges

through truncated lozenges, {100}-bounded leaf-shape crystals, to highly elongated needles at the growth rate minimum. This is the exact reversal of the sequence observed in polyethylene.[1] As discussed in ref 14, this sequence is associated with increasing self-poisoning and may help explain the T_c dependence of crystal morphology in polyethylene.

Acknowledgment. The authors are indebted to Drs. G. M. Brooke, S. Mohammed, S. Burnett, and D. Proctor of Durham University for providing the long alkanes $C_{162}H_{326}$ and $C_{198}H_{398}$. We acknowledge financial support from Petroleum Research Fund, administered through the American Chemical Society, and from the Engineering and Physical Science Research Council.

References and Notes

(1) Organ, S. J.; Keller, A. *J. Mater. Sci.* **1985**, *20*, 1571.
(2) Toda, A. *Polymer* **1991**, *32*, 771.
(3) Bassett, D. C.; Olley, R. H.; Al-Raheil, A.-M. *Polymer* **1988**, *25*, 1539.
(4) Toda, A. *Faraday Discuss.* **1993**, *95*, 129.
(5) Keith, H. D. *J. Appl. Phys.* **1964**, *35*, 3115.
(6) Khoury, F. *Faraday Discuss. Chem. Soc.* **1979**, *68*, 404.
(7) Sadler, D. M. *Polymer* **1983**, *24*, 1401.
(8) Mansfield, M. L. *Polymer* **1988**, *29*, 1755.
(9) Point, J. J.; Villers, D. *J. Cryst. Growth* **1991**, *114*, 228.
(10) Frank, F. C. *J. Cryst. Growth* **1974**, *22*, 233.
(11) Cheng, S. Z. D.; Chen, J. *J. Polym. Sci., Part B: Polym. Phys.* **1991**, *29*, 311.
(12) Organ, S. J.; Keller, A.; Hikosaka, M.; Ungar, G. *Polymer* **1996**, *37*, 2517.
(13) Ungar, G.; Mandal, P. K.; Higgs, P. G.; de Silva, D. S. M.; Boda, E.; Chen, C. M. *Phys. Rev. Lett.* **2000**, *85*, 4397.
(14) Ungar, G.; Putra, E. G. R.; Mandal, P. K.; de Silva, D. S. M., submitted for publication.
(15) de Silva, D. S. M.; Ungar, G., manuscript in preparation.
(16) Higgs, P. G.; Ungar, G. *J. Chem. Phys.* **2001**, *114*, 6958.
(17) Brooke, G. M.; Burnett, S.; Mohammed, S.; Proctor, D.; Whiting, M. C. *J. Chem. Soc., Perkin Trans. 1* **1996**, 1635.
(18) Organ, S. J.; Ungar, G.; Keller, A. *Macromolecules* **1989**, *22*, 1995. Hobbs, J. K.; Hill, M. J.; Keller, A.; Barham, P. J. *J. Polym. Sci., Part B: Polym. Phys.* **1999**, *37*, 3188. Mandelkern, L.; Prasad, A.; Alamo, R. G.; Stack, G. M. *Macromolecules* **1990**, *23*, 3696.
(19) Passaglia, E.; Khoury, F. *Polymer* **1984**, *25*, 631.
(20) Ungar, G.; Keller, A. *Polymer* **1987**, *28*, 1899.
(21) Higgs, P. G.; Ungar, G. *J. Chem. Phys.* **1994**, *100*, 640.
(22) Tanzawa, Y.; Toda, A. *Polymer* **1996**, *37*, 1621.

MA010146Y